Riverine biogeochemistry from the Andes to the ocean: longitudinal patterns along a Mediterranean Andean catchment in central Chile

Morgane Derrien[1*], Simona Retelletti Brogi[2,3], Céline Lavergne[4,5], Zoé Hayet[1], Mario Flores[6], Fernando Lizana[7], Polette Aguilar-Muñoz[5,8], Leo Chasselin[9], Chiara Santinelli[3]

[1]BioGeoQuím Lab, Instituto de Ciencias Agroalimentarias, Animales y Ambientales, Universidad de O'Higgins, San Fernando, 3007000, Chile
[2]Istituto Nazionale di Oceanografia e di Geofisica Sperimentale, Trieste, 34010, Italy
[3]Consiglio Nazionale delle Ricerche (CNR), Istituto di Biofisica, Pisa, 56124, Italy
[4]Department of Physiology, Genetics and Microbiology, University of Alicante, San Vicente del Raspeig, 03690, Spain
[5]HUB AMBIENTAL UPLA and Departamento de Ciencias y Geografía, Universidad de Playa Ancha, Valparaíso, 2340000, Chile
[6]Carrera de Pregrado Ingeniería Ambiental, Universidad de O'Higgins, San Fernando, 3007000, Chile
[7]Magíster de Ciencias Ambientales y de la Tierra, Instituto de Ciencias Agroalimentarias, Animales y Ambientales (ICA3), Universidad de O'Higgins, Rancagua, 2820000, Chile
[8]Centro de Investigación Oceanográfica COPAS COASTAL, Universidad de Concepción, Concepción, 3349001, Chile
[9]Centre de Recherches en Environnement Côtier, Université de Caen, Luc-sur-Mer, 14530, France

Correspondence to: Morgane Derrien (morgane.derrien@uoh.cl)

Abstract. Rivers act as dynamic connectors between terrestrial and marine ecosystems, transporting and transforming materials along the aquatic continuum. We investigated longitudinal biogeochemical patterns across the Rapel catchment (central Chile) by integrating dissolved organic matter (DOM) characterization, dissolved metals and nutrients, and microbial community profiling from the Andean headwaters to the Pacific Ocean. Headwaters were characterized by low DOC and nutrient concentrations, high protein-like fluorescence, and diverse microbial assemblages dominated by Flavobacterium, Polaromonas, and Rhodoferax. Downstream, agricultural and mining activities increased nutrient and metal concentrations and altered microbial community composition with an increasing prevalence of hgcI_clade. The Rapel Reservoir emerged as a major biogeochemical discontinuity, promoting DOM transformation, restructuring microbial assemblages, and modifying downstream chemical conditions. Overall, tributary inputs, land use, and hydrological regulation disrupted simple longitudinal patterns and generated distinct biogeochemical processing zones. These findings highlight the interplay between downstream transport and local processing in shaping riverine functioning in Mediterranean Andean catchments and provide a basis for assessing future climate and land-use impacts on riverine biogeochemistry.

1 Introduction

Rivers act as dynamic connectors between terrestrial and marine ecosystems, transporting to the ocean dissolved organic matter (DOM), nutrients, metals, and microbes derived from soils, groundwater, tributaries, and in-stream production, all of which are continuously transformed along the aquatic continuum (Doretto et al., 2020; Wollheim et al., 2022). These transformations

regulate freshwater quality, ecosystem functioning, and the export of carbon and nutrients from continents to the ocean, linking inland processes with regional and global marine biogeochemical cycles (Aufdenkampe et al., 2011; Regnier et al., 2022; Ward et al., 2017). Riverine biogeochemistry is not indeed regulated solely by downstream transport. It emerges from the continuous interaction between hydrology, landscape connectivity, biological activity, and local environmental conditions operating along the longitudinal continuum, from mountain headwaters to the estuarine interface, where sources, transport, and transformation processes remain tightly coupled.

The River Continuum Concept (RCC) offers a useful framework for interpreting longitudinal patterns in riverine biogeochemistry (Vannote et al., 1980). The RCC postulates that the structure and function of river ecosystems change predictably along the continuum, reflecting shifts in hydrology, energy sources, and biotic interactions (Ortiz Muñoz and Kominoski, 2025; Ruiz-González et al., 2015). Headwaters (i.e., low-order streams) are typically dominated by allochthonous inputs of organic matter and strong hydrological control, whereas downstream reaches become progressively influenced by in-stream production and transformation processes. These changes may be reflected in the quantity and composition DOM, as terrestrial organic matter inputs are progressively transformed and supplemented by autochthonous production downstream, as well as in nutrient concentrations and availability through uptake, transformation, and remineralization (Graeber et al., 2012; Fovet et al., 2020). Similarly, longitudinal changes in metal concentrations and mobility may result from differences in lithology, dilution, tributary inputs, redox conditions, and anthropogenic sources, while microbial diversity and community composition may respond to changes in organic matter quality, nutrient availability, and physicochemical conditions along the river network (Lu and Yu, 2018; Mayol et al., 2026). Although this conceptual model remains fundamental to limnology, increasing evidence suggests that many contemporary river systems deviate from this idealized continuum due to hydrological regulation, land-use change, and anthropogenic disturbance (Doretto et al., 2020; Roebuck et al., 2020). In catchments, watersheds, reservoirs, tributary inflows, agricultural runoff, anthropogenic activities, and urban pressure can introduce abrupt discontinuities in physicochemical conditions and material transport (Poole, 2002; Ellis and Jones 2013; Stanford and Ward, 1983; Ward and Stanford 2001). These discontinuities may alter DOM composition, nutrient cycling, metal mobility, and microbial community dynamics, effectively reshaping downstream biogeochemical functioning. As a result, river systems may behave less as linear continua and more as mosaics of interconnected biogeochemical processing zones. Recent conceptual theories, including the river as a chemostat (Creed et al., 2015), the Pulse-Shunt Concept (Raymond et al., 2016), and the bending DOM framework (Casas-Ruiz et al., 2020), increasingly emphasize the importance of hydrological variability, residence time, and localized processing hotspots in controlling riverine carbon and nutrient dynamics along the fluvial gradient.

Despite these advances, integrative studies simultaneously examining organic matter composition, inorganic chemistry, and microbial diversity across complete river continua remain limited (Bambakidis et al., 2024; Regnier et al., 2022). Such integrative approaches are essential for capturing the spatial and temporal complexity of riverine biogeochemistry and assessing how natural gradients and anthropogenic pressures jointly shape biogeochemical fluxes across entire watersheds or catchments (Amaral et al., 2016; Kothawala et al., 2020).

In this study, we investigated the longitudinal biogeochemical dynamics of the Rapel catchment in central Chile, a large Andean-to-coastal Mediterranean ecosystem covering ~~approximately 14,000~~ 13,700 km². The basin encompasses strong altitudinal and hydrological gradients, contrasting land uses, intense agricultural (mainly in the Tinguiririca subcatchment) and mining activities (strongly influencing the Cachapoal subcatchment, Lacassie and Ruiz-Del-Solar (2021)), and the presence of one of the largest reservoirs in central Chile (Rapel subcatchment, Bravo-Linares et al. (2024)). Together, these characteristics make the Rapel catchment an ideal system to explore the interplay among natural environmental gradients, anthropogenic pressures, and hydrological regulation interact to shape riverine biogeochemistry along the aquatic continuum. To address this objective, we combined DOM characterization, dissolved metal and nutrient analyses, together with microbial community profiling based on 16S rRNA gene metabarcoding across the catchment, from the Andean headwaters to the estuarine outlet. Rather than considering these compartments independently, we aimed to evaluate how DOM, inorganic chemistry, and microbial community structure co-vary along the river continuum and how these relationships are influenced by environmental conditions, land use, and flow regulation. Because several discontinuities were identified in the Rapel catchment, we hypothesized that the conventional RCC model may have limited validity in this system. Specifically, we hypothesized that, rather than showing smooth gradients from headwaters to the estuary, the catchment would exhibit pronounced shifts driven by hydrological conditions and anthropogenic pressures. The objectives of this study were to (1) characterize the longitudinal dynamics of DOM concentration and composition from upstream to downstream sectors; (2) assess spatial variations in microbial community diversity and composition along the continuum; and (3) better understand the coupled biogeochemical-microbial interactions at the catchment scale. By integrating these multiple dimensions across the entire catchment, this study provides new insights into the functioning of regulated Mediterranean climate Andean rivers and into how anthropogenic pressures reshape riverine biogeochemical organization from the headwaters to the coastal ocean.

2 Material and Methods

2.1 Study area

The Rapel catchment is located in central Chile (34°S-71°W) within the Libertador General Bernardo O'Higgins Region, covering approximately 13,700 km², which corresponds to almost the entire region, extending from the high Andes to the Pacific Ocean. Its strong altitudinal gradient, with elevations ranging from over 5,000 m a.s.l. (above sea level) in the eastern Andean headwaters to sea level at the coast, generates marked climatic and ecological contrasts, encompassing glacial areas, mountain ranges (The Andes and the Coastal Cordillera, respectively), steep valleys, agricultural plains, and coastal lowlands (Cornwell et al., 2020). The Rapel catchment is formed by the confluence of the Cachapoal and Tinguiririca rivers and drains westward into the Rapel Reservoir (artificial reservoir) and then via the Rapel River it reaches the Pacific Ocean at Navidad. The total fluvial length from the headwaters to the mouth is approximately 310 km.~~, after 310 km, in Navidad~~. The climate is Mediterranean-temperate, with a prolonged dry summer (November-March) and cold winters (May-August). Annual precipitation varies between 450 and 1,050 mm, falling mostly during the austral winter as snow above ~1,500 m a.s.l. and

rain at lower elevations (Bennison et al., 2021). Interannual variability in precipitation is high and influenced by large-scale climatic modes such as the El Niño–Southern Oscillation (ENSO), making the system particularly sensitive to climate change and long-term shifts in precipitation regimes (Jaksic, 1998). Hydrologically, the catchment has a mixed snow–rain regime, with snowmelt and rainfall driving seasonal flow variations. Average annual discharges recorded between 1981 and 2010 for the main tributaries of the Cachapoal and Tinguiririca Rivers are 89.0 m^3/s and 50.2 m^3/s, respectively (DGA, 2015). Once ~~re~~united in the Rapel Reservoir (695 Mm^3), one of Chile's largest artificial lakes, the water discharge is regulated for hydropower generation, irrigation, and domestic use. These characteristics of the catchment create a strong spatial heterogeneity in water chemistry and ecological conditions along the longitudinal continuum. Land use follows the altitudinal gradient. The upper Andean zone (i.e., above 2000 m a.s.l.) is sparsely populated, and vegetation is largely absent (~18% of the total area). ~~At lower elevations~~ Below 2,000 m a.s.l., native vegetation communities predominate along the Andean slopes and foothills, including forest and grazing lands (~25%). Further downstream, the middle and lower reaches support intensive agricultural activities, including vineyards, fruit orchards, and croplands, which are sustained by irrigation networks and livestock farming (~50% of the total area) (Fig. S1). The catchment also hosts significant mining operations, particularly in the upper area of the Cachapoal River (>0.5%), where the largest underground copper mine is located, which contributes to metal inputs and potential contamination (Copaja et al., 2016; Lacassie and Ruiz del Solar, 2021). In contrast, the two main cities of the region (i.e., Rancagua and San Fernando) and the downstream sectors are increasingly influenced by urban and recreational developments associated with the Rapel Reservoir and coastal zone (~5%) (Fig. S1) (CONAF, 2024; Cornwell et al., 2020).

~~To examine the complete river continuum, 25 sampling sites were selected along the catchment, from the Andes to its mouth in Navidad (Fig. 1), of which 11 were within the Cachapoal subcatchment (hereinafter station name beginning with C , i.e., C-C1), 8 within the Tinguiririca subcatchment (hereinafter station name beginning with T , i.e., T-T1), and 6 within the Rapel subcatchment (hereinafter station name beginning with R , i.e., R-R1).~~ To examine the complete river continuum, 25 sampling sites were selected along the catchment, from the Andes to its mouth in Navidad (Fig. 1). Of these, 11 sites were located within the Cachapoal subcatchment, 8 within the Tinguiririca subcatchment, and 6 within the Rapel subcatchment. Station names follow a standardized nomenclature in which the first letter indicates the subcatchment (C = Cachapoal, T = Tinguiririca, and R = Rapel), while the following letter(s) identify the river within the corresponding subcatchment, followed by the station number, when applicable. For example, C-C1 refers to sampling point 1 on the Cachapoal River within the Cachapoal subcatchment, whereas C-P refers to the sampling point on the Portillo River within the Cachapoal subcatchment. Thus, the station code provides information on both the subcatchment and the river where the sampling site is located. The choice of the sites aimed to represent the main streams and tributaries in order to capture the riverine biogeochemistry along the longitudinal gradient (e.g., headwaters, transition zone, and floodplain). In addition to considering confluences, land-use changes, and topographic variability, only sites with easy access and moderate elevation were chosen to minimize fieldwork constraints. To represent the spatial dynamics of the measured parameters in a reader-friendly representation, a reference site was chosen as spring of the Tinguiririca and Cachapoal rivers according to the lowest reach of the two glaciers that originate them (located

from satellite images), in the results some data are therefore presented in function of the distance from the glacier base (Km). The main tributaries are plotted in correspondence of their confluence with the main river. The confluence of the two rivers into the Rapel Reservoir is approximately at the same distance from the two glaciers (140 - 145 Km), it was therefore decided to consider it to be 145 Km distant from both glaciers.

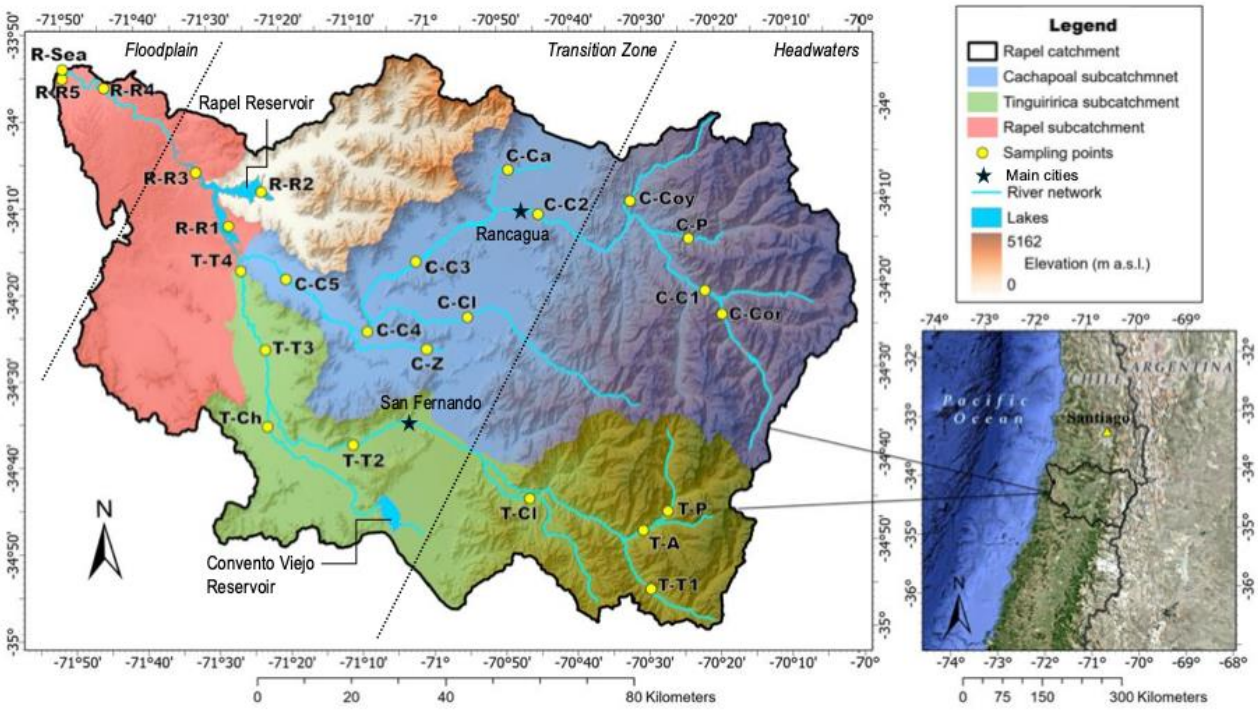


Figure 1 - Map of the study area and its location in Chile. Sampling site locations and names are indicated on the map. Station names beginning with C- indicate the samples collected within the Cachapoal subcatchment (blue area in the map). Station names beginning with T- indicate the samples collected within the Tinguiririca subcatchment (green area in the map). Station names beginning with R- indicate the samples collected within the Rapel subcatchment (red area in the map).

2.2 Samples collection

The sampling campaign was conducted between 13 and 22 November 2024 (spring in the Southern Hemisphere). Physico-chemical parameters (temperature, pH, dissolved oxygen (DO), and electrical conductivity normalized to 25 °C (EC)~~, and total dissolved solids (TDS)~~ were measured in situ at each site using a Hanna HI 98194 multiparametric probe (Hanna Instruments, Italy). Nitrates were also measured in situ using a TriOS OPUS probe (TriOS Mess- und Datentechnik GmbH, Germany). Water samples were collected into 1 L HCl-cleaned polycarbonate bottles (Nalgene) and filtered on-site using a Sterivex filter (0.22 µm, polyethersulfone). Subsamples of the filtrate were collected, after three rinses, into: 40 mL pre-combusted glass

vials for dissolved organic carbon (DOC) analyses; 250 mL HCl-cleaned polycarbonate bottles (Nalgene) for measuring DOM fluorescence (FDOM) and total dissolved nitrogen (TDN); 100 mL HNO_3 cleaned HDPE bottles for the determination of metals and metalloids. The filters were used for the microbial diversity analyses. Samples for DOC and metals were immediately acidified using Sovrapure HCl and HNO_3, respectively. All the water samples were conserved in a cooler and finally stored at 4°C upon returning to the laboratory, within the day. Sterivex filters were stored frozen at −20 °C for a few weeks to a maximum of 4 months before extraction.

2.3 ~~Samples collection~~ Analytical measurements

The analyses for DOC and TDN were carried out through high temperature combustion (HTC) method by using a TOC-L analyzer (Shimadzu corporation, Japan) equipped with a TN module following the SOPs of Halewood et al. (2022). The measurement's reliability was verified daily using consensus reference material (CRM; (Hansell, 2005) - CRM batch n° 02-23, MSR nominal concentration 55-57 µM C and 6-7 µM N) at the beginning and at the end of each sample's run.

Metals, metalloids, and some nonmetals (S and P) were measured on pre-acidified filtered samples (SW-846 Test Method 3005A, EPA) using an inductively coupled plasma to optical emission spectrometry (ICP-OES, iCAP Pro, ThermoScientific, USA).

Tridimensional Excitation-Emission Matrices (EEMs) of fluorescence were measured using an Aqualog spectrofluorometer (Horiba, Japan) with excitation ranging from 250 to 450 nm (5 nm interval) and emission ranging from 212 to 620 nm (0.8 nm interval). The TreatEEM software (Omanovic et al., 2023) was used to remove the Rayleigh and Raman scatter peaks and to normalize fluorescence to Raman Units (R.U.). Parallel Factor Analysis (PARAFAC) was carried out by using the drEEM toolbox (Murphy et al., 2013). A 4-component model was validated (98.9% explained variance, Fig. S2) and the components were compared with similar components reported in the literature using the OpenFluor database (Murphy et al., 2014) and attributed to specific groups of fluorophores (Table S1; C1mh: Marine Humic-like, C2th: Terrestrial Humic-like; C3p: Protein-like, C4p: Protein-like).

2.4 Microbial diversity

Microbial DNA was extracted from the collected Sterivex filters. The filters were thawed on ice and opened under sterile conditions in a laminar flow hood using a scalpel that had been disinfected with 70% ethanol and exposed to UV light. The filter was divided in half; one half was stored as a backup in a cryotube, while the other half was used for extraction with the DNeasy PowerSoil Pro kit (QIAGEN, USA) according to the manufacturer's protocol, with elution in 50 µL.

The extracted DNA was quantified using the Qubit 4 Fluorometer (Thermo Fisher Scientific, USA), using the Qubit dsDNA HS Assay kit (Thermo Fisher Scientific, USA). A verification PCR was performed to ensure the quality of the extracted DNA. Briefly, the 16S rRNA gene was amplified using the following primers: EUB1 (GAGTTTGATCCTGGCTCAG, (Liesack et al., 1991)) and 519R (GTATTACCGCGGCKGCTG, (Lane, 1991)). The PCR mix for each sample consisted of: 13.3 µL of ultrapure water, 5 µL of Green Buffer 5X (Promega, USA), 3 µL of $MgCl_2$ (Thermo Scientific, USA), 0.5 µL of dNTPs

(Thermo Scientific, USA), 0.5 µL of the forward primer (EUB1), 0.5 µL of the reverse primer (519R), 0.2 µL of Taq polymerase (Thermo Scientific, USA), and 2 µL of the extracted DNA (previously diluted if the concentration exceeded 5 ng/µL). The PCR program was run in an Aeris thermocycler under the following conditions: an initial denaturation step at 95 °C for five minutes, followed by 35 cycles of denaturation at 95 °C for 40 seconds, hybridization at 57 °C for 40 seconds, elongation at 72 °C for 40 seconds, and a final extension at 72 °C for five minutes. Metabarcoding sequencing was performed using an Illumina NovaSeq 6000 PE250 at Novogene with in-house primers 515F (GTGYCAGCMGCCGCGGTAA) and 806R (GGACTACNVGGGTWTCTAAT) for the V4 region of the 16S rDNA gene, based on the work of Caporaso et al. (2011).

The sequencing yielded an average of 186,002 ± 45,669 raw reads per sample. The amplicon sequence variants (ASVs) were generated and checked for chimeras using the DADA2 pipeline (Callahan et al., 2016) in QIIME2 (v. 2019.7; (Bolyen et al., 2019)). This process resulted in an average of 155,640 ± 37,086 reads per sample and retained ~~XX%~~ 83.9 ± 3.6% of the raw reads. Representative sequences obtained were used for taxonomic assignment, which was performed by comparing the 16S rRNA gene sequences with the SILVA database version 138.2 database (SSU NR99, full-length sequences; (Quast et al., 2013)), using the *classify-consensus-vsearch* method (Rognes et al., 2016). The generated nucleotide sequences were deposited in the public database NCBI under the Bioproject PRJEB114990 and accession numbers ranging from ERR17408622 to ERR174086.

2.5 Statistical analysis

All the statistical analyses were performed in R version 4.5.1 (R Core Team, 2013) using the graphical interface R Studio version 2026.01.2+418. Significant differences of physicochemical parameters among subcatchments were assessed using Kruskal Wallis test due to non-normal distribution of the data, followed by a Wilcoxon rank sum exact test for pairwise comparison using the Holm method for p-value adjustment. Significant trends along the watercatchment were determined using the spearman correlation between the distance from the glacier base and the tested parameter; note that spearman correlation was chosen after a multivariate normality test (*mvn* function, 'MVN' package; Korkmaz et al., 2014). A PERMANOVA was used to identify the significant difference of the metal and metalloids studied among the different subcatchments. The dispersion within groups was tested using the *betadisper* function ('vegan' package (Oksanen et al., 2007)), and pairwise multilevel comparisons were assessed using the *pairwise.adonis* function ('pairwiseAdonis' package; (Arbizu, 2020)) with the Bonferroni P correction. The microbial diversity dataset was processed and analyzed using the "phyloseq" package (McMurdie and Holmes, 2013). Standard filters were applied at this stage to improve the dataset's quality, including removing singletons and taxa classified as unassigned (at the domain level), chloroplast, or mitochondria. The matrix was then normalized by rarefaction to 65,000 sequences per sample, and three samples with fewer sequences were removed from the database. The ecological analyses described in the following section were performed using this filtered, normalized matrix. Alpha diversity was assessed using the observed richness, Chao1, Shannon, and Simpson indices and beta diversity was analyzed using Bray-Curtis distances and PCoA ordinations. For alpha diversity indexes, significant differences between

subcatchment (i.e., Cachapoal, Tinguiririca, and Rapel) or between catchment levels (i.e., headwaters, transition zone, floodplain) were determined through one-way ANOVA and Tukey HSD post-hoc test if assumptions were confirmed. When assumptions were not confirmed, the Kruskal-Wallis rank sum test was used, associated with the Dunn test (P was adjusted with the Benjamini-Hochberg method). A multiple factor analysis (MFA) was performed (*MFA* function, 'FactomineR' package; (Husson et al., 2013)) to explore the relationship between microbial composition, metals and metalloids, environmental variables, and components of DOM; field triplicates were used as observations ($n = 60$). The variables included in each group have been selected by forward selection using the *forward.sel* function on the standardized matrices. In consequence, the group matrices are composed as follows: Physicochemistry, 4 variables (pH, Conductivity, temperature, dissolved oxygen); Organic Matter, 4 variables (C1mh, C2th, C3p, C4p); Metals, 16 variables (Al, P, As, Mo, Cd, B, Mn, Fe, Mg, Cr, V, Cu, Ag, Ba, Li, K). The matrix of the microbial composition was built with the 78 most abundant ASVs (>10% of the total community considering all samples). Before performing the MFA, the variables were scaled to unit variance. To prevent bias, the elevation was only added as a supplementary quantitative variable, not used to build the ordinations. Similarly, for representation purposes, the three subcatchments and the three catchment levels were added as supplementary qualitative variables.

All numerical data supporting this study have been deposited in the Zenodo repository and will be publicly accessible upon publication.

3 Results

3.1 In situ physicochemical conditions

Across the whole study area, water temperature spanned from 8.6 °C (T-T1) to 23.12 °C (R-R3) (Table S2). The lowest temperatures (>12°C) were observed in the headwaters, followed by a progressive increase along the longitudinal gradient, with the highest values (>23°C) recorded at sampling points located within the Rapel Reservoir. ~~Salinity values remained low (<0.4) across most sampling sites within the catchment (Table S2).~~ pH ranged from 5.97 to 8.90, with most sites exhibiting circumneutral to slightly alkaline conditions (7.30–8.10). The lowest pH was recorded at C-Coy (5.97), possibly due to nearby mining activities, whereas the highest value was recorded at R-R2 (8.90), within the Rapel Reservoir (Table S2). Dissolved oxygen (DO) concentrations varied between 4.46 and 11.5 mg/L. The lowest DO was measured at the Cadenas creek (C-Ca = 4.46 mg/L), while the highest concentration was observed in the Rapel Reservoir at R-R2 (11.5 mg/L). Most stations showed well-oxygenated conditions (>8 mg/L) (Table S2). Electrical conductivity (EC) ranged from 39 µS/cm (T-Cl) to 2513 µS/cm at the marine-influenced site (R-Sea). No consistent longitudinal trend was observed, as relatively elevated values (e.g., >500 µS/cm) occurred both in upstream and downstream sections of the catchment. The Tinguiririca subcatchment ~~generally~~ significantly displayed the lowest EC values (Pairwise comparisons, $P < 0.05$). ~~Total dissolved solids (TDS) ranged from 19 to 1264 mg/L, with maximum concentrations at the sea-influenced site (R-Sea) and intermediate values (135–376 mg/L) across most continental stations.~~ Nitrate (NO_3^-) concentrations displayed pronounced spatial variability, ranging from 4.0 µM (T-Cl)

to 274.7 µM (C-Z). Elevated nitrate concentrations were recorded in the Cachapoal subcatchment downstream, particularly at C-C4 (193.3 µM), C-Cl (142.7 µM), and C-C5 (127.8 µM) (Table S2).

3.2 DOC and TDN concentration

Dissolved organic carbon (DOC) over the entire study area ranged from 9 to 213 µM. The lowest DOC concentrations were observed in samples collected in the Andes Mountains, with concentrations significantly increasing downstream (Fig. 2a; Spearman correlation with the distance from the glacier: $\rho = 0.79$, $P < 0.05$, Fig. S3). In the Cachapoal River, the concentration was 14 µM in the high mountain (C-C1) and increased after 75 km downstream of the site, following the input of Cadenas and Zamorano creeks (C-Ca and C-Z), which had 205 and 120 µM of DOC, respectively. In the Tinguiririca River, DOC concentration increased gradually from 11 µM at the highest point of the subcatchment to 60 µM before reaching the Rapel Reservoir. Its main tributaries showed similar DOC concentrations as the main river, except Chimbarongo Creek (T-Ch), which had a slightly higher DOC concentration (70 µM). Within the Rapel Reservoir, DOC reached the highest concentration (213 µM in R-R2) and slowly decreased downstream to 56 µM at the estuary. Total dissolved nitrogen (TDN; Fig. 2b) ranged between 7 and 329 µM. The lowest concentrations were observed in the Andes mountains and increased moving downhill. In the Cachapoal River, the lowest concentration (9 µM) was observed in the mountains (C-Cor) and increased after 75 km to reach a markedly higher concentration in the C-C4 site (235 µM). The maximum concentration of TDN was observed in the Zamorano Creek (C-Z, 329 µM). In the Tinguiririca River, TDN increased gradually from 10 to 52 µM, and within its main tributaries, the Chimbarongo had a higher concentration (T-Ch, 60 µM). Within the Rapel Reservoir (R-R1 and R-R2), TDN showed lower values (ranging between 28 and 38 µM) with respect to the Cachapoal and Tinguiririca inputs into the lake and increased again downstream the reservoir toward the sea.

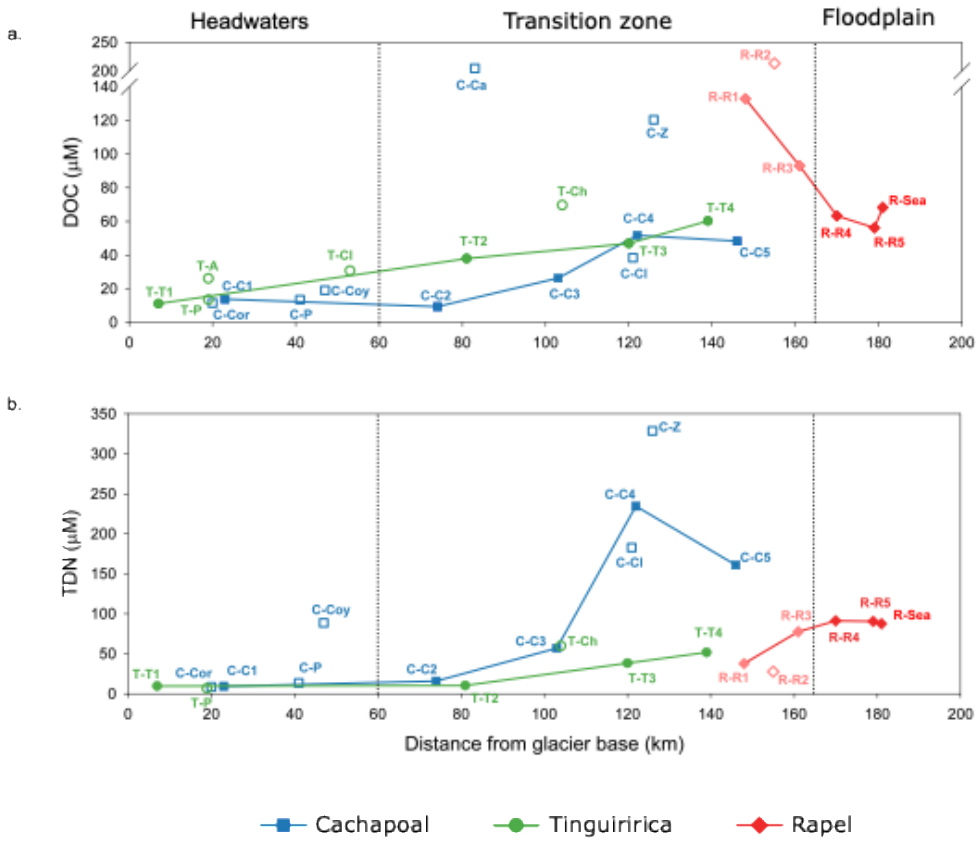


Figure 2: Dissolved Organic Carbon (DOC) concentration (a) and Total Dissolved Nitrogen (b) in the three subcatchments. Line and scatter plots (with filled symbols) represent the main rivers while open symbols represent the tributaries. In the Rapel subcatchment, the reservoir sample is shown in a lighter shade. The code names of the sampling sites are shown next to the corresponding dots. Note that the y-axis of DOC concentration has a break between 140 and 200 µM due to the marked difference between the concentration in C-Ca and R-R2 and the rest of the sites, helping in highlighting the concentration dynamics in the lower concentration sites.

3.3 DOM optical properties

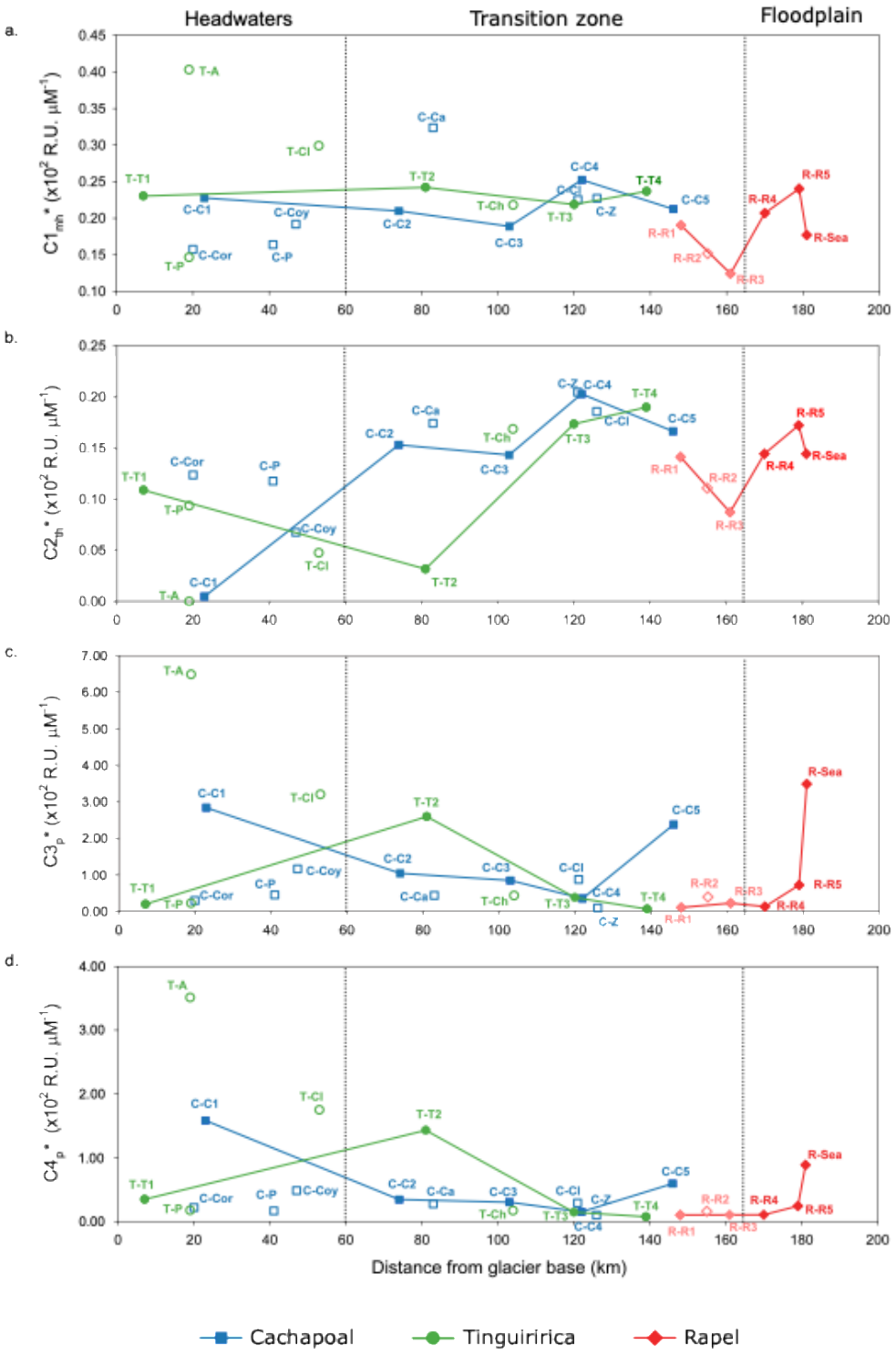
The PARAFAC analysis of the EEMs and comparison of the results within the Openfluor database (Table S2) resulted in the identification of two humic-like and two protein-like components. C1mh (λEx/λEm max: 315/409 nm) has characteristics that are usually attributed to humic-like compounds that have been reprocessed by the microbial community. C2th (λEx/λEm max: 260(365)/469 nm) has the typical excitation and emission maxima attributed to terrestrial humic-like compounds. C3p

(λEx/λEm max: 300/348 nm) has fluorescence maxima that resemble those of protein-like compounds in water, i.e., tryptophan, but its excitation maximum occurs at longer wavelengths than the typical protein-like components of DOM. This suggests that its fluorescence may be influenced by factors such as being bonded within bigger molecules or complexed with metals (Aiken, 2014). Interestingly this component was found to be more than 98% similar (Openfluor comparison) to components identified in other regions affected by the presence of ice (Chen et al., 2018; Maurischat et al., 2022). C4p (λEx/λEm max: 275/338 nm) fluorescence maxima are those usually related to protein-like fluorescence.

The percentage of each component of total fluorescence (as the sum of the four components) was calculated and showed that in 21 of 25 stations, the percentage of protein-like components (C3p + C4p) fluorescence was predominant (>50%) with respect to the humic-like components (C1mh + C2th), reaching up to 96% of total fluorescence (station T-A). Only stations C-Z, T-T4, R-R1, and R-R4 showed a predominance of humic-like components, having the maximum of 76% in T-T4 (Table S1).

To account for the large variability in DOC concentrations across the study area and because of the concentration dependence of fluorescence signals, FDOM patterns within the catchment were characterized using concentration-normalized fluorescence. Normalized fluorescence gives information on the changes in DOM optical properties regardless of the concentration. Therefore, the fluorescence of each component in each sample was divided by the DOC concentration of that sample. To improve figures readability and sample's fluorescence data easily comparable, the values of the normalized fluorescence was multiplied by 10^2 and therefore reported as 10^{-2} R.U. μM^{-1}. The normalized components are indicated by the addition of an asterisk in the components' name (e.g., $C1_{mh}$*).

The microbial humic-like C1mh* showed little variation in the two main rivers, Chachapoal and Tinguiririca, ranging between 0.19 and 0.25 x 10^{-2} R.U. μM^{-1}, and no spatial trend was observed (Fig. 3a). The tributaries showed more variability, ranging from 0.15 to 0.40 x 10^{-2} R.U. μM^{-1}, with the highest values observed in the Azufre stream. Lower values (< 0.20 x 10^{-2} R.U. μM^{-1}) were observed in the Rapel Reservoir, whereas in the effluent towards the sea, C1mh* values were similar to those of Chachaopal and Tinguiririca. The humic-like C2th* showed a higher variability, having values ranging between 0 and 0.20 x 10^{-2} R.U. μM^{-1} in the entire catchment (Fig. 3b). In the Cachapoal and Tinguiririca main rivers, an increasing trend was observed moving downwards, with the only exception in T-T2, which had lower values. Similarly to C1mh* a decrease in fluorescence was observed within the Rapel Reservoir, while in the floodplain area, C2th* had similar fluorescence to Cachapoal and Tinguiririca in most downstream samples. The protein-like C3p* ranged between 0.06 and 2.84 x 10^{-2} R.U. μM^{-1} in the Cachapoal and Tinguiririca main streams (Fig. 3c). In Cachapoal, a decreasing trend from the headwaters downstream was observed until C-C4, followed by higher values in the C-C5 sampling station. Lower values were observed in the Tinguiririca River, except for T-T2, probably due to elevated inputs from the two tributaries, Azufre (T-A) and Claro (T-Cl). In particular, the Azufre tributary (T-A) showed the highest C3p* value (6.48 x 10^{-2} R.U. μM^{-1}). A marked enrichment was also observed in the sea sample. The tryptophan-like C4p* ranged between 0.07 and 1.58 x 10^{-2} R.U. μM^{-1} in Cachapoal and Tinguiririca main streams and showed a similar trend to that of C3p*, including the maximum value observed in the Azufre tributary (T-A) (Fig. 3d).


a.
b.
c.
d.
Headwaters
Transition zone
Floodplain
$C1_{mh}$ * (x10^2 R.U. µM^{-1})
$C2_{fh}$ * (x10^2 R.U. µM^{-1})
$C3_p$ * (x10^2 R.U. µM^{-1})
$C4_p$ * (x10^2 R.U. µM^{-1})
Distance from glacier base (km)
Cachapoal
Tinguiririca
Rapel

317

Figure 3: Concentration normalized fluorescence of the 4 identified components: microbial humic-likeC1mh* (a), terrestrial humic-like C2th* (b), protein-like C3p* (c), and tryptophan-like C4p* (d) in the three subcatchments. Line and scatter plots (with filled symbols) represent the main rivers while open symbols represent the tributaries. In the Rapel subcatchment, the reservoir sample is shown in a lighter shade. The code names of the sampling sites mentioned within the text are shown next to the corresponding dots.

3.4 Dissolved metals, metalloids, and nonmetals distribution

Dissolved metals and metalloids displayed marked spatial variability across the Rapel catchment (Table S2). Major elements, including Ca, Na, Mg, K, and S, dominated the dissolved fraction at all sampling sites. Calcium remained relatively stable across the catchment, with average values ranging between 17 and 24 ppm, with the lowest values observed in the Tinguiririca subcatchment, particularly at its headwaters (T-A = 13.569, T-P = 12.403, and T-Cl = 5.164 ppm). By contrast, Na, Mg, and K displayed pronounced variability across the catchment, with the highest concentrations recorded at the river–ocean interface (R-Sea: Na = 79.169 ppm, Mg = 22.378 ppm; K = 13.890 ppm). Sulfur concentration was also elevated at the interface R-Sea (49.829 ppm), although the highest values were observed at specific inland sites, namely C-Coy (99.744 ppm) and R-R2 (51.145 ppm).

Within the Cachapoal subcatchment, C-Coy was characterized by elevated concentrations of Cu (4.710 ppm), potentially ~~confirming the influence of~~ related to the upstream copper mining activities in this tributary, as well as Mn (2.168 ppm) and Zn (0.796 ppm). C-Ca exhibited the highest P concentration (0.384 ppm), likely reflecting the influence of agricultural activities in the surrounding area. These two sites displayed distinct metal signatures compared to the rest of the catchment. Notably, the Tinguiririca subcatchment displayed overall lower concentrations of dissolved metals and metalloids (Pairwise multilevel comparison associated with PERMANOVA; $P < 0.05$; Tables S3 & 4), but without following a clear longitudinal pattern. In contrast, the Rapel subcatchment stations (R-R1 to R-R5) generally presented intermediate metal concentrations for most elements, except for R-R2, which exhibited some of the highest concentrations of major elements within the catchment (e.g., Ca, Na, Mg, K, and S), and where Mo was detected with the highest concentration (0.041 ppm).

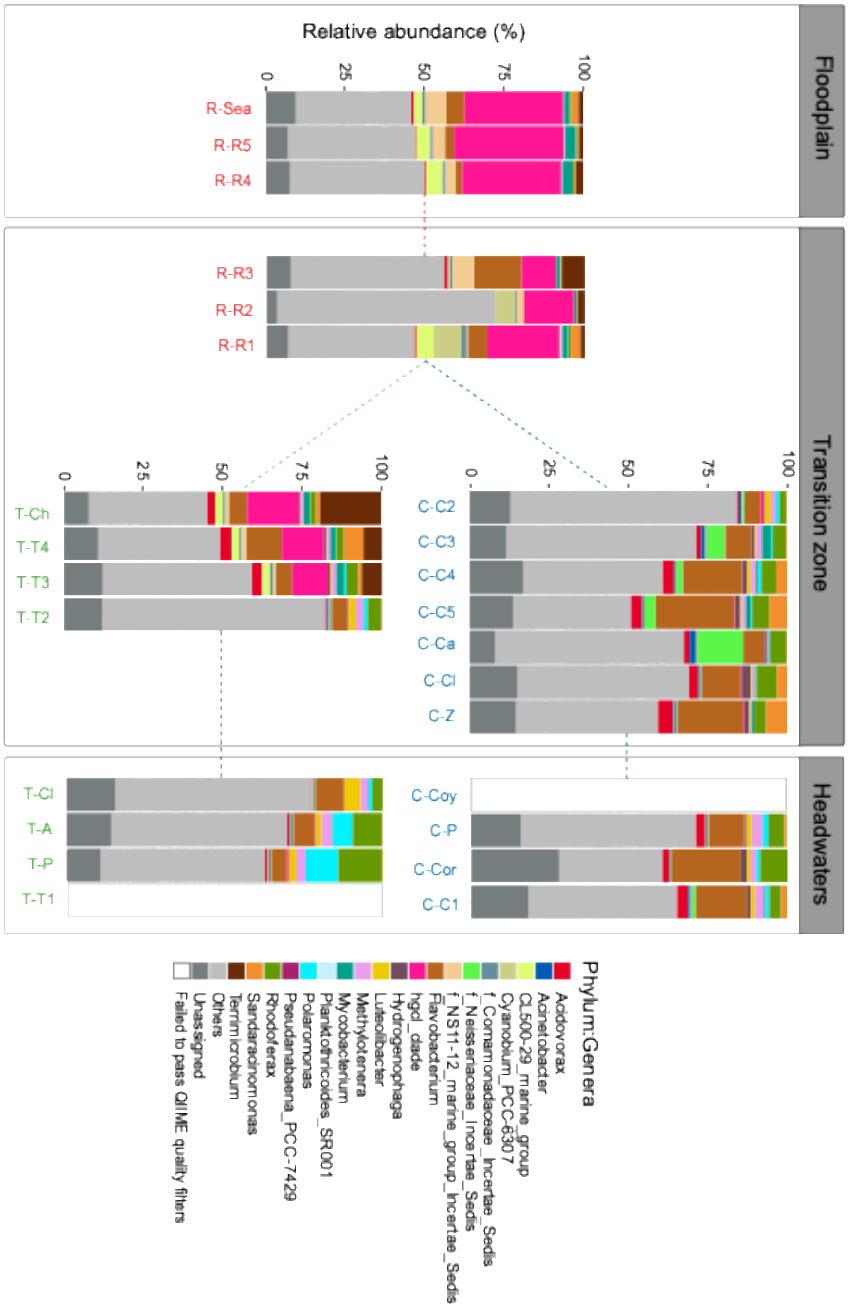
3.5 Microbial community structure and diversity patterns

The taxonomic composition of microbial communities varied markedly along the catchment, across altitudinal zones and subcatchments, while maintaining a recurrent core set of genera present throughout the system (Fig. 4). In the headwater areas, community structure was relatively diverse as indicated by high Shannon index values (Fig. 5), with several abundant genera co-occurring across sites. Flavobacterium, Luteolibacter, and Rhodoferax were widely distributed and in some locations reached or exceeded 20% of total relative abundance. Additional genera, including Polaromonas, Acidovorax, Methylotenera, and Mycobacterium, contributed consistently at lower proportions. A substantial fraction of total abundance corresponded to taxa grouped as “Others” (approximately 33–61%), representing genera outside the 20 most abundant taxa and reflecting a composition along the catchment distributed across multiple lineages. In the transition zone of the catchment, community

structure was more heterogeneous, with pronounced differences among subcatchments. Flavobacterium maintained elevated abundances at several sites, in some cases exceeding 20% in the Cachapoal subcatchment. Other taxa, including hgcI_clade, Terrimicrobium, CL500-29_marine_group, Cyanobium_PCC-6307, and Sandaracinomonas, contributed substantially at specific locations (i.e., Tinguiririca and Rapel subcatchments), indicating spatially structured shifts in dominance. This variability was mirrored in the wide range of the "Others" fraction, which exceeded 60% at several sites, suggesting high compositional turnover within this section of the catchment.

In contrast, the ~~lower~~ floodplain zone of the catchment exhibited a more strongly dominated community structure as revealed by lower Chao1 (Dunn test; $Z= 2.53$ and -2.47 for headwaters and transition zone, respectively; $P < 0.05$) and Shannon (Dunn test; $Z= 3.14$ and -2.50 for headwaters and transition zone, respectively; $P < 0.05$) indexes compared to the headwaters and the waters from the transition zone (Fig. 5a). The hgcI_clade emerged as the most representative taxon, consistently exceeding 30% relative abundance. Although Flavobacterium, CL500-29_marine_group, Terrimicrobium, and Mycobacterium remained present, their contributions were comparatively lower.

At the subcatchment scale, the Cachapoal subcatchment displayed relatively diverse communities with moderate abundances distributed among multiple genera, including Flavobacterium, Rhodoferax, Acidovorax, Sandaracinomonas, Methylotenera, and Mycobacterium. Tinguiririca subcatchment appeared comparatively balanced, with consistent contributions from Flavobacterium, Rhodoferax, Luteolibacter, Polaromonas, and Sandaracinomonas, as well as moderate proportions of Terrimicrobium and hgcI_clade, without a single overwhelmingly dominant genus as confirmed by high Shannon values. In contrast, the Rapel subcatchment exhibited lower Chao and Shannon indexes compared to other subcatchments (Tukey HSD, $P < 0.05$, Fig. 5b), characterized by the predominance of hgcI_clade and notable contributions from CL500-29_marine_group, Cyanobium_PCC-6307, Terrimicrobium, and Mycobacterium, particularly in lacustrine sectors (R-R1, R-R2, and R-R3).



370

371 **Figure 4: Microbial community composition and diversity indexes. Relative abundance of the 20 most abundant**
372 **microbial genera retrieved from the 16S gene metabarcoding dataset along the catchment levels (Headwaters,**

Transition zone, Floodplain) and across the three subcatchments (C - Cachapoal, T - Tinguiririca, and R - Rapel). Note that when Genera was not defined, Family is used and the name of the taxonomic group starts by "f_".

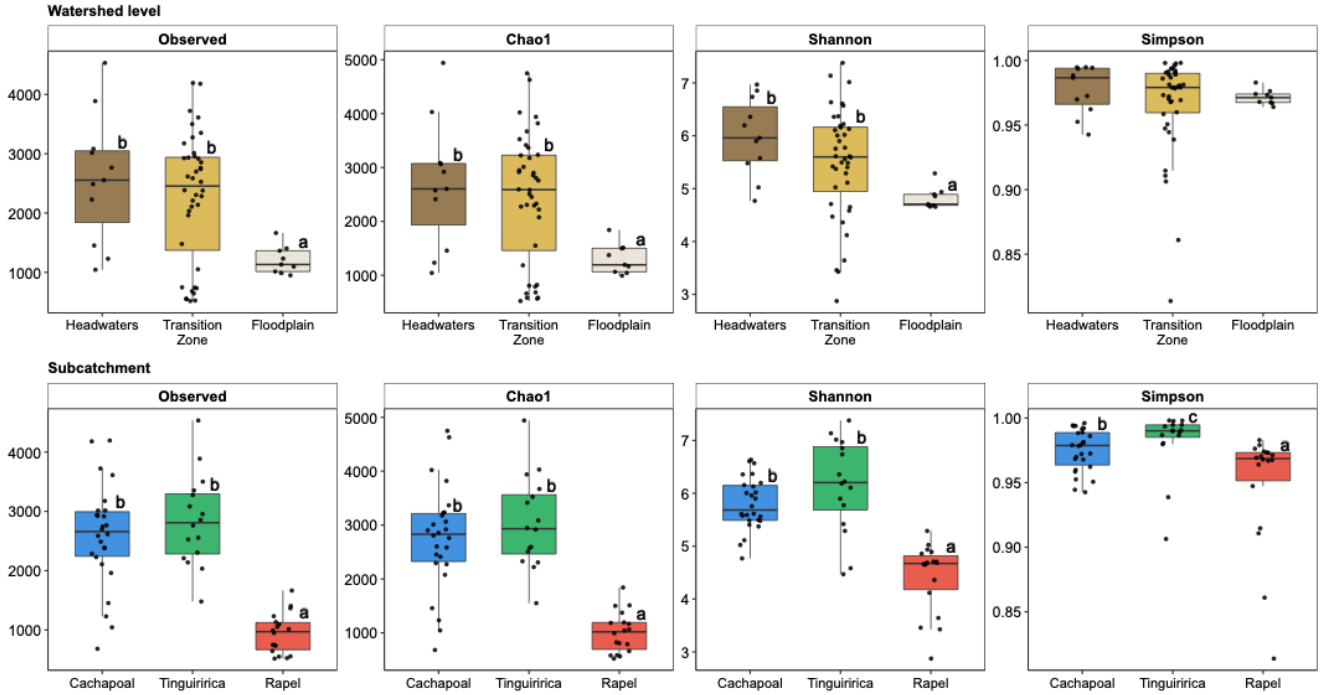


Figure 5: Alpha diversity indices (Observed richness, Chao1, Shannon, and Simpson) across catchment levels (headwaters, transition zone, and floodplain) (a) and subcatchments (b) during the spring season. Boxplots illustrate the distribution of alpha diversity metrics among samples collected at each spatial category, highlighting variations in microbial community richness and diversity along the longitudinal organization of the catchment. Letters indicate significant differences assessed through one-way ANOVA and Tukey HSD post-hoc tests if assumptions were confirmed. When assumptions were not confirmed, the Kruskal-Wallis rank sum test was used, associated with the Dunn test considering the adjusted P with the Benjamini-Hochberg method ($P < 0.05$).

3.6 Multivariate relationships among microbial, geochemical, and DOM variables

The MFA allowed visualization of how the river samples clustered based on their biogeochemical signatures, including physicochemical parameters, FDOM, prokaryotic community structure, and metal and metalloid concentrations (Fig. 6a). Together, the first three dimensions of the ordination represent 47.6% of the variation. The first dimension of the MFA discriminated well between the different subcatchments and the catchment levels (e.g., headwaters, transition zone, and floodplain) (Fig. 6b and d). It was mainly characterized by conductivity, temperature, Mg, and V, as well as Chitinophagaceae Sediminibacterium and the hgcI_clade bacteria (Fig. 6c). The second dimension allowed the separation of most transition zone

samples from the other catchment levels. This second dimension was defined mainly by the C1mh and C2th humic-like components, B, Li, Sphingomonadaceae Sphingorhabdus, and Microbacteriaceae Rhodoluna bacteria (Table S6, Dim2). Interestingly, the third dimension was mainly built by pH, Mo concentrations, and the protein-like components C3p and C4p. Along this third MFA dimension, high values of the C3p and C4p components were associated with a greater abundance of Cyanobacteria, including the filamentous taxa Leptolyngbyaceae Calothrix and Phormidiaceae Planktothrix, as well as Microcystaceae Microcystis and Cyanobiaceae Cyanobium PCC-6307 (Table S7, Dim3).

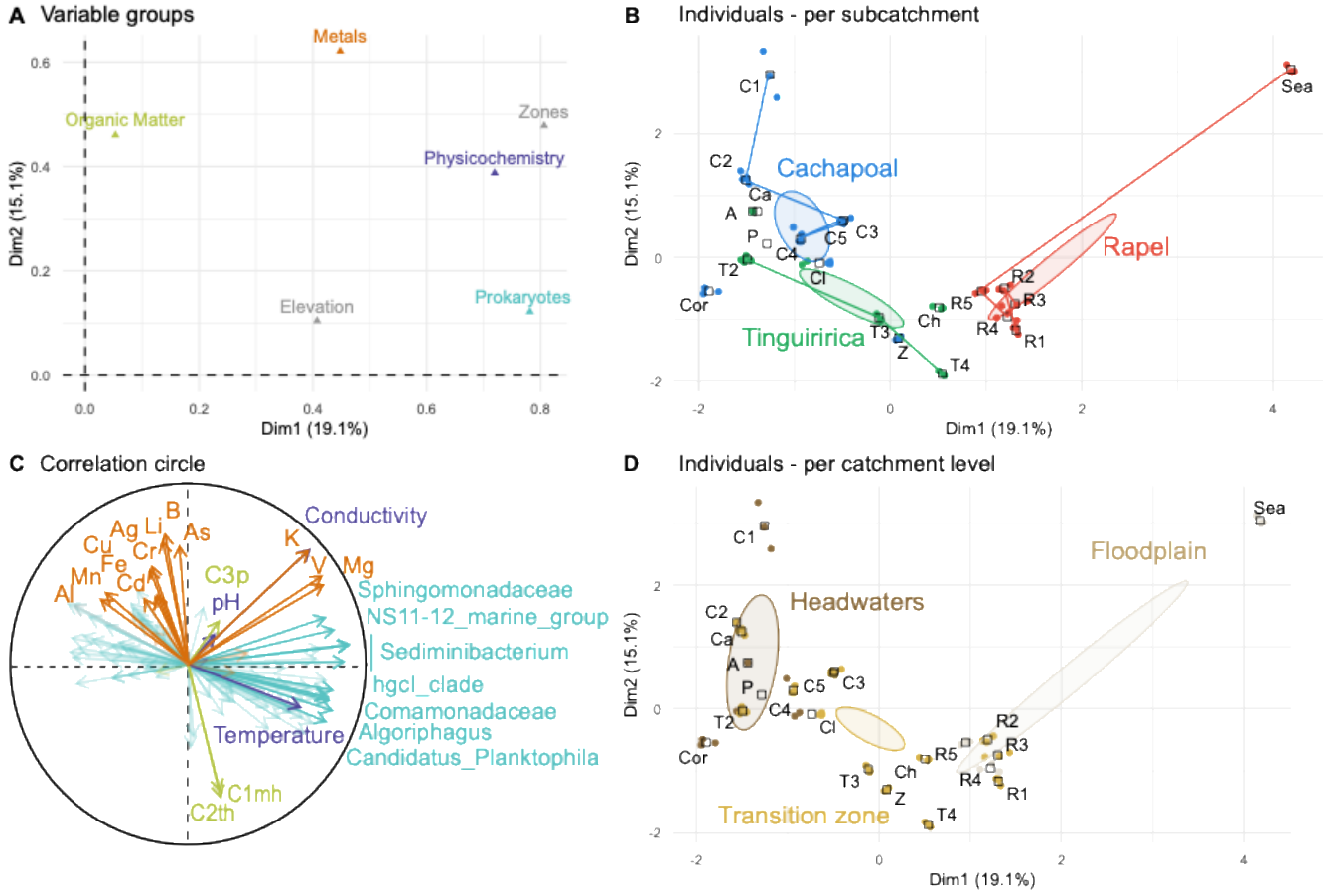


Figure 6: Multiple factor analysis built with the microbial composition, metals and metalloids, environmental variables, and components of DOM. Coordinates of each group, the supplementary groups are plotted in grey (a); Individual coordinates on the ordination (Dimension 1 & 2) colored by subcatchment (b), note that the line represents the main stream path from the highest elevation to the lowest within each subcatchment; Correlation circle from the first two dimensions and considering only the 30 variables with higher contributions (c); Individual coordinates on the ordination (Dimension 1 & 2) colored by catchment levels (d). Note that for (b) and (d) panels, the points represent all the replicates and the open squares are the barycenter of the replicates. The ellipses are confidence ellipses at 95%.

4 Discussion

4.1 Longitudinal co-variance of organic, inorganic, and biological compartments and the relationship with the land use

The Rapel catchment exhibited a strong longitudinal pattern of in DOC (Fig. 2), FDOM (Fig. 3), dissolved inorganic chemistry (Table S2), and microbial communities (Fig. 4), reflecting the combined influence of natural geomorphological gradients and contrasting land-use pressures across the Andes-to-ocean continuum. Along the river network, the changes in these biogeochemical variables were not independent but rather covaried spatially, revealing coupled processes operating at the catchment scale, as shown by the MFA (Fig. 6).

The headwater sectors of both Andean subcatchments (i.e., Cachapoal and Tinguiririca) were characterized by cold, well-oxygenated waters with low DOC, TDN, NO_3^- concentrations, and EC, except for the Coya stream (C-Coy), likely due to its location downstream of copper mining activities. These conditions are typical of high-altitude mountain systems, where sparse vegetation cover, limited soil organic matter accumulation, and strong hydrological connectivity with cryospheric and groundwater sources exert dominant controls on riverine biogeochemistry (Maurischat et al., 2022; Singer et al., 2012; Tanguang et al., 2015). FDOM instead showed unexpectedly high fluorescence of the two protein-like components, C3p and C4p, across most upstream sampling points (Fig. 3; e.g., more than 10 times higher fluorescence intensities of the protein-like components compared to the humic ones). This very high fluorescence suggests that DOM was dominated by in situ-produced and possibly labile organic matter in these environments. This is in agreement with the dominance of protein-like fluorescence in small Chinese rivers during spring (Shi et al. 2024), where one of the driving factors of water quality was nitrate concentration. Protein-like fluorescence in high mountains can also be derived from glaciers and snowmelt (Drapeau et al., 2025; Dubnick et al., 2022). Indeed, there is strong evidence supporting the in situ production of organic matter, particularly protein-like compounds, by photoautotrophic microorganisms within glaciers (Anesio et al., 2009; Maurischat et al., 2022) or also sea ice (Retelletti Brogi et al., 2018; Stedmon et al., 2011). On one side, and as also reported from field and experimental studies, the highest C3p* and C4p* values coincided with the greatest abundance of cyanobacteria, including Cyanobium PCC-6307 (Li et al., 2025; Tedetti et al., 2026; Yin et al., 2025). Most of the cyanobacteria retrieved were likely not free-living but instead associated with Nostoc cyanobacterial mats observed on stream rocks (Hentschke et al., 2025). Cyanobacterial mats act as a dynamic environment where both organic matter produced and microorganisms can be retrieved in the water and play an important role that may be considered in future research (Scott and Marcarelli, 2012).

On the other side, the extremely high C3p* and C4p* values observed in the Azufre tributary (T-A, Fig. 3c and d) may be also likely related to its distinctive origin within volcanic and hydrothermal-influenced environments associated with the Tinguiririca volcanic complex, as observed also in the marine environment (Tedetti et al., 2026 and references therein). These previous studies attribute the high protein-like fluorescence to biological production (i.e., chemosynthesis) or abiotic factors which are promoted by the elevated temperature. The humic-like compounds might instead be more easily thermally degraded (Tedetti et al., 2026). Higher values of the BIX fluorescence index, indicating a higher contribution of *in-situ* produced DOM was also found in a volcanic site compared to a reference area (Retelletti Brogi et al., 2019). Abiotic production of DOM at

increasing temperature was also demonstrated in laboratory-controlled experiments (Lin et al., 2017). Finally, we cannot exclude the anthropogenic contribution to the protein-like FDOM pool, in agreement with Liu et al. (2026), which recently reported the dominance of protein-like DOM (average approx. 70%) along a small river impacted by mining.

Despite small differences in dissolved metal concentrations and microbial community composition between the upper locations of both subcatchments, their overall biogeochemical fingerprints remained similar. These headwater ~~upstream~~ environments displayed characteristics commonly associated with relatively pristine Andean headwaters, including limited anthropogenic influence and strong controls exerted by lithology, cryospheric processes, and mountain hydrology on water chemistry and microbial organization, ~~where shared lithology, cryosphere weathering, and mountain hydrology appear to exert the primary controls on water chemistry and microbial organization~~, as has also been observed in other high-mountain regions (e.g., Alpine and Tibetan headwaters) (Brighenti et al., 2026; Garcia et al., 2018; Hotaling et al., 2017; Maurischat et al., 2022).

Moving downstream, the transition zones of both subcatchments showed the clearest influence of anthropogenic land use on the river's biogeochemistry. These sectors were characterized by the accumulation of nutrients, dissolved ions, metals, and organic matter, together with shifts in microbial community composition. Elevated NO_3^- concentrations coincided with increases in DOC, TDN, EC, and dissolved metal concentrations, particularly downstream of tributaries influenced by agricultural activities (Fig. S1). For example, the Cadenas tributary (C-Ca) exhibited elevated phosphorus concentrations (Table S2), likely associated with agricultural runoff and diffuse inputs from surrounding cultivated areas. These chemically distinct tributaries disrupted simple longitudinal gradients and generated localized biogeochemical "hotspots" within the river network. In parallel, the transition sectors were characterized by a progressive increase in the C2th* humic-like component (Fig. 3b), reflecting the accumulation of terrestrial organic matter along the river continuum.

The influence of these transition zones was also evident in the microbial communities, although the response differed between the two subcatchments. The simultaneous enrichment in nutrients, dissolved ions, and DOC in these impacted sectors was also accompanied by clear shifts in microbial community composition relative to the upstream headwaters. The Cachapoal subcatchment, for instance, was characterized by the occurrence of Betaproteobacteria Neisseriaceae family within the Cadenas tributary (C-Ca), a bacterial group that can be found in freshwater environments but which also includes genera associated with wastewater and anthropogenic contamination (de Santana et al., 2025). In the present case, its occurrence may be linked to effluent discharges from the wastewater treatment plant located a few kilometers upstream. In contrast, the Tinguiririca subcatchment showed a more pronounced shift in microbial organization, characterized by the increased abundance of hgcI_clade and Terrimicrobium. Terrimicrobium has frequently been associated with surrounding agricultural soils and may reflect terrestrial inputs into the aquatic system, whereas hgcI_clade represents one of the most abundant and ubiquitous groups of free-living planktonic bacteria in inland waters worldwide (Wang et al., 2024). Its high relative abundance in these sectors may also reflect the changing nutrient conditions along the transition zone (Ghylin et al., 2014).

Further downstream, the Rapel Reservoir represented a major biogeochemical transition zone within the catchment, functioning both as a sink and an active reactor for organic and inorganic constituents. DOC reached its highest concentration within the reservoir, whereas humic-like fluorescence decreased relative to upstream sectors, indicating substantial in-reservoir

transformation of DOM with the removal of the terrestrial humic-like fraction through processes such as photochemical degradation and microbial remineralization. This dynamic has been observed in other regulated rivers where the presence of dams resulted in an increase in DOC concentration and/or a higher relative abundance of in-situ produced DOM such as protein-like fluorescence (Acharya et al., 2023, He et al., 2025; Zhuang et al., 2023). Simultaneously, microbial community composition shifted toward the dominance of hgcI_clade and an increased presence of lacustrine-associated taxa such as CL500-29_marine_group (Wang et al., 2024). The microbial composition within the reservoir was similar to the Tinguiririca transition zone, suggesting a strong microbial and biogeochemical influence from the Tinguiririca inflow. The local enrichment of taxa such as Terrimicrobium, Sandaracinomonas, and Cyanobium within the transition sectors likely reflects the increasing influence of nutrient-enriched conditions, total dissolved solids, longer water residence times, and flow regulation associated with agricultural landscapes (Cabello-Yeves et al., 2018; Pitt et al., 2024; Qiu et al., 2017). In parallel, the accumulation of major ions and several dissolved elements at R-R2 (Table S2) suggests that hydrological retention and internal biogeochemical cycling contribute to solute enrichment within the lacustrine system, potentially due to its external input from the Alhue stream. This is a small stream coming from outside the Rapel catchment that flows into the Rapel reservoir next to the R-R2 sampling site.

Downstream of the reservoir, the floodplain and the estuarine sectors reflect the continuing influence of these major hydrological and biogeochemical transitions, while also showing distinct downstream characteristics. ~~Together, these patterns indicate that the reservoir and its upstream transition zones act as areas of intensified ecological and biogeochemical transformation within the aquatic continuum, decoupling local biogeochemical dynamics from simple upstream–downstream transport.~~ The floodplain samples are a reflection of the reservoir pattern for most of the biogeochemical variables. By contrast, the estuarine interface displays a unique fingerprint due to the seawater input (Anderson and Harvey, 2022; Zhang et al., 2025). Together, these patterns indicate that the reservoir and its upstream transition zones act as areas of intensified ecological and biogeochemical transformation within the aquatic continuum, decoupling local biogeochemical dynamics from simple upstream–downstream transport.

Overall, the entire Rapel catchment demonstrates that longitudinal riverine organization emerges from the interaction between natural altitudinal gradients, hydrological connectivity, and anthropogenic land use. DOC, FDOM, dissolved inorganic compounds, and microbial community structure displayed coherent spatial covariation, highlighting the existence of tightly interconnected biogeochemical compartments along the aquatic continuum (Fig. 6). Rather than behaving as isolated components, DOM, dissolved inorganic compounds, and microbial assemblages responded synchronously to shifts in environmental conditions and land use, from oligotrophic Andean headwaters to agriculturally and mining-influenced transition zones, reservoir processing environments, and estuarine interface. These findings reinforce the importance of integrated catchment-scale approaches to understand how natural and anthropogenic pressures jointly regulate riverine biogeochemical functioning in Mediterranean Andean catchments.

4.2 Rethinking the river continuum concept and its application in riverine biogeochemistry

The River Continuum Concept proposed by Vannote et al. (1980) remains one of the foundational frameworks in limnology for understanding the longitudinal organization of river ecosystems. The RCC predicts that gradual downstream changes in channel morphology, hydrology, light availability, and energy sources should drive corresponding and relatively predictable shifts in organic matter composition, nutrient processing, and biological community structure. Within this framework, headwaters are typically characterized by strong terrestrial influence and heterotrophic processing. In contrast, downstream, sections progressively shift toward finer organic matter, greater autochthonous production, and altered community composition as materials are transformed along the continuum (Guo et al., 2025; Kamjunke et al., 2026). Microbial communities are also expected to vary along the river continuum in response to shifts in organic matter sources, nutrient availability, and environmental conditions (Ruiz-González et al., 2015). Headwaters generally sustain diverse microbial assemblages adapted to heterogeneous and dynamic environments, whereas downstream communities progressively shift toward taxa associated with more stable, productive, and internally regulated conditions (Ezzat et al., 2025; Mayol et al., 2026). However, microbial diversity does not necessarily follow a simple linear downstream pattern (Tan et al., 2025). It may instead be highest in intermediate reaches of the river network, where increased environmental heterogeneity and mixing of water sources promote greater ecological and functional diversity (Laperriere et al., 2020; Mayol et al., 2026).

Our results from the entire Rapel catchment partially support these expectations, particularly in the upper Andean headwaters, but beyond these upper reaches, the system ~~Rapel catchment~~ departed markedly from the progressive and predictable longitudinal organization proposed by the RCC. Instead of a smooth downstream transition, DOM, dissolved metals, nutrients, and microbial communities were strongly reorganized by tributary inputs, land use, and hydrological regulation. Mining-affected tributaries (mainly affecting the Cachapoal river, Lacassie et al. (2021)) introduced localized enrichments in Cu, Mn, Zn, sulfate, and NO_3^-, while agricultural sectors contributed elevated nutrient inputs. These anthropogenic inputs generated biogeochemical discontinuities that disrupted any simple continuum-driven organization and created spatially heterogeneous "hotspots" of processing within the river network.

The Rapel Reservoir represented the strongest discontinuity within the system and fundamentally altered downstream biogeochemical trajectories. Increased residence time within the reservoir promoted DOC accumulation, shifts in DOM fluorescence, and major changes in microbial community composition, including the dominance of lacustrine-associated taxa such as hgcI_clade and CL500-29_marine_group. Simultaneously, the reduction in humic-like fluorescence and the persistence of protein-like signatures suggest changes in the DOM pool that can be explained by autochthonous production, microbial processing, photodegradation, and sedimentation. In this context, the reservoir did not simply interrupt the river continuum physically; the dam effectively fragmented the fluvial system and reset downstream chemical and biological conditions, generating a new biogeochemical baseline for downstream reaches. In addition, hydrological regulation downstream of the dam modified discharge variability and residence time, further limiting the expression of natural longitudinal patterns (Liu et

al., 2022). Together with tributary inflows and anthropogenic inputs from agricultural and mining sectors, these processes generated spatially heterogeneous hotspots of biogeochemical processing across the river network.

These findings show that although the RCC remains a valuable conceptual framework, its predictive power is limited in regulated and anthropogenically impacted river systems (Doretto et al., 2020; Roebuck et al., 2020). In Mediterranean Andean catchments such as the studied one, riverine biogeochemistry appears to be structured not only by longitudinal transport but also by major biogeochemical control points, including reservoirs, tributary confluences, anthropogenic disturbances, floodplains, and estuarine interfaces (Danczak et al., 2023; Jones, 2010). Our results, therefore, support a more dynamic view of the river continuum, where hydrological regulation, land use, and localized processing can override expected continuum-driven organization. Even the recent alternative conceptual approaches, such as the river as a chemostat (Creed et al., 2015), the Pulse–Shunt Concept (Raymond et al., 2016), and the Bending DOM framework (Casas-Ruiz et al., 2020), which take into account variability, regulation, and localized processing, are not fully able to represent the patterns observed in the Rapel catchment. Nonetheless, these theories emphasize the need for more comprehensive studies to understand the processes along the river continuum. Indeed, the results of this study suggest that the organization of riverine biogeochemistry in the Rapel catchment emerges from the interaction between hydrology, land use, local environmental conditions, and internal processing across different sectors of the catchment.

Finally, the observed dynamics within the Rapel catchment highlight the potential sensitivity of Mediterranean-Andean rivers to the combined influence of land-use and hydrological pressures and suggest how these systems ~~Mediterranean-Andean rivers may~~ respond to increasing environmental pressures. ~~under increasing climate and land-use pressure.~~ Within our study area, biogeochemical patterns varied along the catchment in association with differences in land use, with some sites showing distinct characteristics in areas where specific anthropogenic activities occur (e.g., Coya and Cadenas Creeks, C-Coy and C-Ca). These observations are consistent with previous studies highlighting the importance of land use as a key factor shaping riverine biogeochemistry (Williams et al., 2010; Maurischat et al., 2023). Beyond these local pressures, regional changes in climate and hydrology may further modify the functioning of such systems. Declining snow cover and glacier retreat have been documented in the Central Andes, together with changes in river discharge and snowmelt contributions (Ohlanders et al., 2013; Ragetti et al., 2016; Masiokas et al., 2020). Although these longer-term climatic and hydrological changes cannot be assessed directly from our dataset, they provide an important context for considering how future changes in water availability may interact with existing land-use pressures and reservoir regulation in Mediterranean-Andean rivers. ~~Reduced snowpack, glacier retreat, altered runoff seasonality, and increasing dependence on reservoirs are likely to strengthen hydrological regulation and further disrupt natural continuum dynamics.~~

4.3 Implications for the riverine biogeochemistry comprehension

One of the main implications of this study is that DOM dynamics cannot be interpreted independently of microbial and inorganic processes. Variations in DOC concentration and FDOM were closely associated with changes in dissolved metals and microbial community composition, suggesting strong interactions between DOM, microbial communities, and

geochemical conditions. In particular, the predominance of protein-like fluorescence across most stations contrasts with the classical view of progressively humified riverine DOM along the downstream continuum. Instead, our observations suggest that a fraction of DOM is produced in situ throughout the catchment, including in high-altitude sectors. These findings suggest that Andean headwaters and cryosphere-influenced environments may represent important sources of organic matter to downstream ecosystems, potentially sustaining microbial activity and carbon processing along the aquatic continuum.

More broadly, the strong spatial heterogeneity observed across the Rapel catchment indicates that longitudinal biogeochemical organization cannot be explained by downstream transport alone. The upper Andean headwaters were distinct from the transition and floodplain sectors, while tributary confluences, land-use transitions, the reservoir, and the estuarine interface represented additional zones of biogeochemical change. This ~~study~~ reinforces the idea that river corridors are active components of regional carbon and nutrient cycling rather than passive conduits linking terrestrial and marine ecosystems. ~~The strong spatial heterogeneity observed across the Rapel catchment indicates that biogeochemical transformations are intensified at ecological transition zones such as tributary confluences, reservoirs, floodplains, and estuarine interfaces. These sectors likely contribute disproportionately to DOM transformation, nutrient recycling, and microbial processing at the catchment scale.~~ In this context, elevation, stream position, hydrological connectivity, and local environmental conditions interact to shape the sources, transformation, and transport of organic and inorganic matter along the catchment.

The timing of sampling also provides an important context for interpreting these spatial patterns. The November campaign was conducted shortly after the onset of the snowmelt period according to DGA (The General Water Directorate) hydrological records (https://mapas2.mop.gob.cl/). Snowmelt may therefore have contributed to the hydrological conditions observed in the upper Andean zone by increasing connectivity between cryosphere-influenced headwaters and downstream reaches. However, because this study covers a single annual cycle and does not include sampling before and throughout the snowmelt period, its specific contribution to the observed biogeochemical patterns cannot be directly quantified. The differences between the upper headwaters and downstream sectors should therefore be interpreted as reflecting the combined influence of seasonal hydrological conditions, elevation, catchment position, tributary inputs, land use, and reservoir regulation rather than as a direct signature of snowmelt alone.

Finally, the results of this study provide a spatial perspective on biogeochemical organization within a strongly heterogeneous Mediterranean-Andean catchment and highlight the potential sensitivity of these systems to future environmental change. ~~have important implications for future climate and land use change scenarios in Mediterranean-Andean regions~~. Glacier retreat, reduced snowpack, and changes in ~~altered~~ runoff seasonality may modify hydrological connectivity, residence time, and DOM sources, while existing land-use pressures and reservoir regulation may further influence these processes. ~~, increasing water demand, and the growing dependence on reservoirs are likely to modify hydrological connectivity, residence time, and DOM sources simultaneously.~~ These changes may alter microbial processing pathways, carbon turnover, nutrient dynamics, and contaminant transport across the aquatic continuum. However, these longer-term changes cannot be assessed directly from our dataset, which covers only a single sampling season. Predicting the future functioning of Andean river systems will therefore require integrated approaches capable of linking hydrology, microbial ecology, organic matter dynamics, and inorganic

geochemistry across the entire catchment, together with multi-year and seasonally resolved observations. ~~Under these future conditions, the role of regulated reservoirs as biogeochemical reactors will likely become even more important in controlling the quantity and quality of material exported downstream. Predicting the future functioning of Andean river systems will therefore require integrated approaches capable of linking hydrology, microbial ecology, organic matter dynamics, and inorganic geochemistry across the entire catchment~~.

5 Conclusion

This study highlights how riverine biogeochemistry in a Mediterranean Andean catchment is structured not only by longitudinal transport along the aquatic continuum, but also by strong local controls associated with land use, tributary inputs, and hydrological regulation. Across the Rapel catchment, DOM concentration and quality, dissolved metals, nutrients, and microbial communities showed strong spatial co-organization, revealing tight coupling between organic, inorganic, and biological compartments.

Headwater sectors retained characteristics typical of oligotrophic Andean systems, whereas downstream sections progressively reflected the influence of anthropogenic activities and reservoir regulation. The Rapel Reservoir emerged as a major biogeochemical discontinuity, substantially reorganizing DOM pool and microbial community structure and effectively resetting downstream biogeochemical conditions.

The study demonstrates that the RCC remains a valuable conceptual framework, but that its predictive capacity becomes limited in highly regulated and anthropogenically impacted systems. In Mediterranean Andean rivers, ecosystem functioning appears increasingly controlled by localized biogeochemical processing zones and hydrological regulation rather than by smooth downstream gradients alone. More broadly, this work emphasizes the need for integrated catchment-scale approaches combining hydrology, microbial ecology, DOM dynamics, and inorganic geochemistry to better understand and predict the functioning of river networks under increasing climate and land-use pressure.

To make a step further in studying the river continuum and to try to relate riverine biogeochemistry to climate, it is paramount to assess both the spatial and the temporal dynamics. This study represents indeed the first step of a larger project which will investigate the spatial dynamics across all seasons and several years.

Code and data availability

Supplementary data to ¨Riverine biogeochemistry from the Andes to the ocean: longitudinal patterns along a Mediterranean Andean catchment in central Chile¨ is made available in the supplement.

Additionally, all numerical data supporting this study have been deposited in the Zenodo repository and will be publicly accessible upon publication (10.5281/zenodo.20753433).

Author contributions

MD: Conceptualization, Data curation, Funding acquisition, Investigation, Methodology, Project administration, Supervision, Validation, Visualization, Writing (original draft preparation), Writing (review and editing). SRB: Conceptualization, Data curation, Formal analysis, Investigation, Methodology, Validation, Visualization, Writing (original draft preparation), Writing (review and editing). CL: Conceptualization, Data curation, Formal analysis, Funding acquisition, Investigation, Methodology, Validation, Visualization, Writing (original draft preparation), Writing (review and editing). ZH: Formal analysis, Data curation, Investigation, Resources, Writing (review and editing). MF: Data curation, Formal analysis, Investigation, Visualization. FL: Data curation, Formal analysis, Investigation. PA-M: Formal análisis, Writing (review and editing). LC: Data curation, Formal analysis. CS: Writing (review and editing).

Competing interests

The authors declare that they have no conflict of interest.

Acknowledgements

~~This work was supported by the Chilean National Agency for Research and Development (ANID) through the Fondecyt grant 1240579. Céline Lavergne was also funded by Marie Curie Postdoctoral Fellowship HORIZON-MSCA-2022-PF-01 #101106387 and acknowledged the institutional support of the "Severo Ochoa Centre of Excellence" accreditation (CEX2024-001494-S). Fernando Lizana acknowledged Pacific Hydro for its scholarship.~~ The authors gratefully acknowledge Pascal Claquin for providing the TriOS OPUS probe used in this study, as well as the owner of Colchagua Glaciares and Miguel Cepeda for granting access to some of the sampling sites. The authors also acknowledge the technical support of Alicia Bruzos from the Centre de Recherche en Environnement Côtier of the Université de Caen, France, and Ignacia Yanten Zuniga, an undergraduate student from the University of O'Higgins, Chile. The authors used ChatGPT (OpenAI) to assist with English language polishing. The authors reviewed and edited all outputs and took full responsibility for the final content.

Financial support

This work was supported by the Chilean National Agency for Research and Development (ANID) through the Fondecyt grant 1240579. Céline Lavergne was also funded by Marie Curie Postdoctoral Fellowship HORIZON-MSCA-2022-PF-01 #101106387 and acknowledged the institutional support of the "Severo Ochoa Centre of Excellence" accreditation (CEX2024-001494-S). Fernando Lizana acknowledged Pacific Hydro for its scholarship.

References

Aiken, G.: Fluorescence and Dissolved Organic Matter, in: Aquatic Organic Matter Fluorescence, edited by: Baker, A., Reynolds, D. M., Lead, J., Coble, P. G., and Spencer, R. G. M., Cambridge University Press, Cambridge, 35–74, https://doi.org/10.1017/CBO9781139045452.005, 2014.

Amaral, V., Graeber, D., Calliari, D., and Alonso, C.: Strong linkages between DOM optical properties and main clades of aquatic bacteria, Limnology and Oceanography, 61, 906–918, https://doi.org/10.1002/lno.10258, 2016.

Anderson, S. R. and Harvey, E. L.: Estuarine microbial networks and relationships vary between environmentally distinct communities, PeerJ, 10, e14005, https://doi.org/10.7717/peerj.14005, 2022.

Anesio, A. M., Hodson, A. J., Fritz, A., Psenner, R., and Sattler, B.: High microbial activity on glaciers: importance to the global carbon cycle, Global Change Biology, 15, 955–960, https://doi.org/10.1111/j.1365-2486.2008.01758.x, 2009.

Aufdenkampe, A. K., Mayorga, E., Raymond, P. A., Melack, J. M., Doney, S. C., Alin, S. R., Aalto, R. E., and Yoo, K.: Riverine coupling of biogeochemical cycles between land, oceans, and atmosphere, Frontiers in Ecology and the Environment, 9, 53–60, 2011.

Bambakidis, T., Crump, B. C., Yoon, B., Kyzivat, E. D., Aho, K. S., Leal, C. F., Fair, J. H., Stubbins, A., Wagner, S., Raymond, P. A., and Hosen, J. D.: Temperature, water travel time, and dissolved organic matter structure river microbial communities in a large temperate watershed, Limnology and Oceanography, 69, 1618–1635, https://doi.org/10.1002/lno.12591, 2024.

Bennison, G., Rojas, R., Claro, E., Bridgart, R., and Caroca, M.: Gestión Integrada de Recursos Hídricos en la Cuenca del Río Rapel. Informe Final (Etapas 1 y 2), 2021.

Bolyen, E., Rideout, J. R., Dillon, M. R., Bokulich, N. A., Abnet, C. C., Al-Ghalith, G. A., Alexander, H., Alm, E. J., Arumugam, M., and Asnicar, F.: Reproducible, interactive, scalable and extensible microbiome data science using QIIME 2, Nature biotechnology, 37, 852–857, 2019.

Brighenti, S., Delpero, M., Bearzot, F., Bertolotti, G., Tolotti, M., Bruno, M. C., Fischer, A., Winkler, G., Voto, G., Aguzzoni, A., Tirler, W., and Comiti, F.: Cryosphere and lithology influence the hydrological gradients of high elevation Alpine catchments, CATENA, 263, 109676, https://doi.org/10.1016/j.catena.2025.109676, 2026.

Callahan, B. J., McMurdie, P. J., Rosen, M. J., Han, A. W., Johnson, A. J. A., and Holmes, S. P.: DADA2: High-resolution sample inference from Illumina amplicon data, Nat Methods, 13, 581–583, https://doi.org/10.1038/nmeth.3869, 2016.

Caporaso, J. G., Lauber, C. L., Walters, W. A., Berg-Lyons, D., Lozupone, C. A., Turnbaugh, P. J., Fierer, N., and Knight, R.: Global patterns of 16S rRNA diversity at a depth of millions of sequences per sample, Proc Natl Acad Sci U S A, 108 Suppl 1, 4516–4522, https://doi.org/10.1073/pnas.1000080107, 2011.

Casas-Ruiz, J. P., Spencer, R. G. M., Guillemette, F., von Schiller, D., Obrador, B., Podgorski, D. C., Kellerman, A. M., Hartmann, J., Gómez-Gener, L., Sabater, S., and Marcé, R.: Delineating the Continuum of Dissolved Organic Matter in Temperate River Networks, Global Biogeochemical Cycles, 34, e2019GB006495, https://doi.org/10.1029/2019GB006495, 2020.

Chen, M., Jung, J., Lee, Y. K., and Hur, J.: Surface accumulation of low molecular weight dissolved organic matter in surface waters and horizontal off-shelf spreading of nutrients and humic-like fluorescence in the Chukchi Sea of the Arctic Ocean, Science of The Total Environment, 639, 624–632, https://doi.org/10.1016/j.scitotenv.2018.05.205, 2018.

CONAF: Actualización del Catastro de los Recursos Vegetacionales y Uso de la Tierra de la Región del Libertador Bernardo O'Higgins. Informe Técnico – Actualización 2020, CONAF, Ministerio de Agricultura, 2024.

Cornwell, E., Sposito, V., and Faggian, R.: Land suitability projections for traditional sub-alpine cropping in the Australian Alps and Chilean Dry Andes. A combined biophysical and irrigation potential perspective, Applied Geography, 121, 102248, https://doi.org/10.1016/j.apgeog.2020.102248, 2020.

Creed, I. F., McKnight, D. M., Pellerin, B. A., Green, M. B., Bergamaschi, B. A., Aiken, G. R., Burns, D. A., Findlay, S. E. G., Shanley, J. B., Striegl, R. G., Aulenbach, B. T., Clow, D. W., Laudon, H., McGlynn, B. L., McGuire, K. J., Smith, R. A., and Stackpoole, S. M.: The river as a chemostat: fresh perspectives on dissolved organic matter flowing down the river continuum, Canadian Journal of Fisheries and Aquatic Sciences, 72, 1272–1285, https://doi.org/10.1139/cjfas-2014-0400, 2015.

Danczak, R. E., Garayburu-Caruso, V. A., Renteria, L., McKever, S. A., Otenburg, O. C., Grieger, S. R., Son, K., Kaufman, M. H., Fulton, S. G., Roebuck, J. A., Myers-Pigg, A. N., and Stegen, J. C.: Riverine organic matter functional diversity increases with catchment size, Front. Water, 5, https://doi.org/10.3389/frwa.2023.1087108, 2023.

DGA: DIAGNÓSTICO DE LA CALIDAD DE LAS AGUAS SUBTERRÁNEAS DE LA REGIÓN, SANTIAGO, report 368, 50, 2015.

Doretto, A., Piano, E., and Larson, C. E.: The River Continuum Concept: lessons from the past and perspectives for the future, Canadian Journal of Fisheries and Aquatic Sciences, 77, 1853–1864, 2020.

Drapeau, H. F., Tank, S. E., Cavaco, M. A., Serbu, J. A., St. Louis, V. L., and Bhatia, M. P.: Shifts in organic matter character and microbial assemblages from glacial headwaters to downstream reaches in the Canadian Rocky Mountains, Biogeosciences, 22, 1369–1391, https://doi.org/10.5194/bg-22-1369-2025, 2025.

Dubnick, A., Faber, Q., Hawkings, J. R., Bramall, N., Christner, B. C., Doran, P. T., Nadeau, J., Snyder, C., Kellerman, A. M., McKenna, A. M., Spencer, R. G. M., and Skidmore, M. L.: Biogeochemical Responses to Mixing of Glacial Meltwater and Hot Spring Discharge in the Mount St. Helens Crater, Journal of Geophysical Research: Biogeosciences, 127, e2022JG006852, https://doi.org/10.1029/2022JG006852, 2022.

Ezzat, L., Peter, H., Bourquin, M., Busi, S. B., Michoud, G., Fodelianakis, S., Kohler, T. J., Lamy, T., Geers, A., Pramateftaki, P., Baier, F., Marasco, R., Daffonchio, D., Deluigi, N., Wilmes, P., Styllas, M., Schön, M., Tolosano, M., De Staercke, V., and Battin, T. J.: Diversity and biogeography of the bacterial microbiome in glacier-fed streams, Nature, 637, 622–630, https://doi.org/10.1038/s41586-024-08313-z, 2025.

Galletti, Y., Gonnelli, M., Retelletti Brogi, S., Vestri, S., and Santinelli, C.: DOM dynamics in open waters of the Mediterranean Sea: New insights from optical properties, Deep-Sea Research Part I: Oceanographic Research Papers, 144, 95–114, https://doi.org/10.1016/j.dsr.2019.01.007, 2019.

Garcia, R. D., Diéguez, M. del C., Gerea, M., Garcia, P. E., and Reissig, M.: Characterisation and reactivity continuum of dissolved organic matter in forested headwater catchments of Andean Patagonia, Freshwater Biology, 63, 1049–1062, https://doi.org/doi:10.1111/fwb.13114, 2018.

Ghylin, T. W., Garcia, S. L., Moya, F., Oyserman, B. O., Schwientek, P., Forest, K. T., Mutschler, J., Dwulit-Smith, J., Chan, L.-K., Martinez-Garcia, M., Sczyrba, A., Stepanauskas, R., Grossart, H.-P., Woyke, T., Warnecke, F., Malmstrom, R., Bertilsson, S., and McMahon, K. D.: Comparative single-cell genomics reveals potential ecological niches for the freshwater acI Actinobacteria lineage, ISME J, 8, 2503–2516, https://doi.org/10.1038/ismej.2014.135, 2014.

Guo, B., Liu, Y., Wang, J., Zheng, Q., Shi, Q., He, C., and Jiao, N.: Environmental and microbial factors shape dissolved organic matter across multiple ecosystems, Commun Earth Environ, 6, 917, https://doi.org/10.1038/s43247-025-02848-3, 2025.

Halewood, E., Opalk, K., Custals, L., Carey, M., Hansell, D. A., and Carlson, C. A.: Determination of dissolved organic carbon and total dissolved nitrogen in seawater using High Temperature Combustion Analysis, Front. Mar. Sci., 9, https://doi.org/10.3389/fmars.2022.1061646, 2022.

Hansell, D. A.: Dissolved Organic Carbon Reference Material Program - Hansell - 2005 - Eos, Transactions American Geophysical Union - Wiley Online Library, 2005.

Hentschke, G. S., Semedo, M., Ciancas, J., Hoepfner, C., Guzmán, D., Rivera, D. S. S., and Vasconcelos, V. M.: Cyanobacterial mats and their associated microbiomes in saline and freshwater lakes from the Bolivian Altiplano, Front. Microbiol., 16, https://doi.org/10.3389/fmicb.2025.1650455, 2025.

Hotaling, S., Hood, E., and Hamilton, T. L.: Microbial ecology of mountain glacier ecosystems: biodiversity, ecological connections and implications of a warming climate, Environmental Microbiology, 19, 2935–2948, https://doi.org/10.1111/1462-2920.13766, 2017.

Husson, F., Josse, J., Le, S., and Mazet, J.: FactoMineR: multivariate exploratory data analysis and data mining with R, R package version, 1, 2013.

Jaksic, F. M.: The multiple facets of El Niño/Southern oscillation in Chile, Revista Chilena de Historia Natural, 71, 121–131, 1998.

Jones, N. E.: Incorporating lakes within the river discontinuum: longitudinal changes in ecological characteristics in stream–lake networks, Can. J. Fish. Aquat. Sci., 67, 1350–1362, https://doi.org/10.1139/F10-069, 2010.

Kamjunke, N., Herzsprung, P., von Tümpling, W., Matoušů, A., Znachor, P., Sanders, T., Brix, H., Bussmann, I., Weitere, M., and Lechtenfeld, O. J.: Longitudinal dynamics and transformation of riverine dissolved organic matter from source to sea, Water Research, 288, 124613, https://doi.org/10.1016/j.watres.2025.124613, 2026.

Kothawala, D. N., Kellerman, A. M., Catalán, N., and Tranvik, L. J.: Organic Matter Degradation across Ecosystem Boundaries: The Need for a Unified Conceptualization, Trends in Ecology & Evolution, 2020.

Lane, D.: 16S/23S rRNA sequencing, Nucleic acid techniques in bacterial systematics, 1991.

Laperriere, S. M., Hilderbrand, R. H., Keller, S. R., Trott, R., and Santoro, A. E.: Headwater stream microbial diversity and function across agricultural and urban land use gradients, Applied and Environmental Microbiology, 86, e00018-20, 2020.

Li, H., Si, D., Wang, H., Jiang, H., Li, P., and He, Y.: Cascading microbial regulation of autochthonous DOM stability in a picocyanobacteria-dominated estuarine reservoir, Water Research, 283, 123752, https://doi.org/10.1016/j.watres.2025.123752, 2025.

Liesack, W., Weyland, H., and Stackebrandt, E.: Potential risks of gene amplification by PCR as determined by 16S rDNA analysis of a mixed-culture of strict barophilic bacteria, Microbial Ecology, 21, 191–198, 1991.

Liu, S., Maavara, T., Yang, X., and Brown, L. E.: Editorial: Riverine Biogeochemistry Under Increasing Damming: Processes and Impacts, Front. Environ. Sci., 10, https://doi.org/10.3389/fenvs.2022.863255, 2022.

Maurischat, P., Lehnert, L., Zerres, V. H. D., Tran, T. V., Kalbitz, K., Rinnan, Å., Li, X. G., Dorji, T., and Guggenberger, G.: The glacial–terrestrial–fluvial pathway: A multiparametrical analysis of spatiotemporal dissolved organic matter variation in three catchments of Lake Nam Co, Tibetan Plateau, Science of The Total Environment, 838, 156542, https://doi.org/10.1016/j.scitotenv.2022.156542, 2022.

Mayol, E., Aguilar-Muñoz, P., Pérez, M., Pavlov, M. S., Rambaldi, G., Eissler, Y., Molina, V., Sola, I., Sáez, C. A., Cuny, P., Heimbürger-Boavida, L.-E., and Lavergne, C.: Microbial community's shifts in an Andean glacier-fed watershed under anthropogenic pressures, Journal of Environmental Management, 404, 129386, https://doi.org/10.1016/j.jenvman.2026.129386, 2026.

McMurdie, P. J. and Holmes, S.: phyloseq: An R Package for Reproducible Interactive Analysis and Graphics of Microbiome Census Data, PLOS ONE, 8, e61217, https://doi.org/10.1371/JOURNAL.PONE.0061217, 2013.

Murphy, K. R., Stedmon, C. A., Graeber, D., and Bro, R.: Fluorescence spectroscopy and multi-way techniques. PARAFAC, Analytical Methods, 5, 6557–6566, https://doi.org/10.1039/C3AY41160E, 2013.

Murphy, K. R., Stedmon, C. A., Wenig, P., and Bro, R.: OpenFluor- an online spectral library of auto-fluorescence by organic compounds in the environment, Analytical Methods, 6, 658–661, https://doi.org/10.1039/C3AY41935E, 2014.

Ortiz Muñoz, L. D. and Kominoski, J. S.: Forecasting climate and human alterations to coastal and estuarine dissolved organic matter, Limnology and Oceanography Letters, 10, 265–286, https://doi.org/10.1002/lol2.70002, 2025.

Quast, C., Pruesse, E., Yilmaz, P., Gerken, J., Schweer, T., Yarza, P., Peplies, J., and Glöckner, F. O.: The SILVA ribosomal RNA gene database project: improved data processing and web-based tools, 2013.

Raymond, P. A., Saiers, J. E., and Sobczak, W. V.: Hydrological and biogeochemical controls on watershed dissolved organic matter transport: Pulse- shunt concept, Ecology, 97, 5–16, https://doi.org/10.1890/14-1684.1, 2016.

Regnier, P., Resplandy, L., Najjar, R. G., and Ciais, P.: The land-to-ocean loops of the global carbon cycle, Nature, 603, 401–410, https://doi.org/10.1038/s41586-021-04339-9, 2022.

Retelletti Brogi, S., Ha, S. Y., Kim, K., Derrien, M., Lee, Y. K., and Hur, J.: Optical and molecular characterization of dissolved organic matter (DOM) in the Arctic ice core and the underlying seawater (Cambridge Bay, Canada): Implication for increased autochthonous DOM during ice melting, Science of the Total Environment, 627, 802–811, https://doi.org/https://doi.org/10.1016/j.scitotenv.2018.01.251, 2018.

Roebuck, J. A. Jr., Seidel, M., Dittmar, T., and Jaffé, R.: Controls of Land Use and the River Continuum Concept on Dissolved Organic Matter Composition in an Anthropogenically Disturbed Subtropical Watershed, Environ. Sci. Technol., 54, 195–206, https://doi.org/10.1021/acs.est.9b04605, 2020.

Rognes, T., Flouri, T., Nichols, B., Quince, C., and Mahé, F.: VSEARCH: a versatile open source tool for metagenomics, PeerJ, 4, e2584, https://doi.org/10.7717/peerj.2584, 2016.

Ruiz-González, C., Niño-García, J. P., Lapierre, J.-F., and del Giorgio, P. A.: The quality of organic matter shapes the functional biogeography of bacterioplankton across boreal freshwater ecosystems, Global Ecology and Biogeography, 24, 1487–1498, https://doi.org/10.1111/geb.12356, 2015.

de Santana, C. O., Spealman, P., Gresham, D., Dueker, M. E., and Perron, G. G.: Bacterial and DNA contamination of a small freshwater waterway used for drinking water after a large precipitation event, Science of The Total Environment, 972, 179010, https://doi.org/10.1016/j.scitotenv.2025.179010, 2025.

Scott, J. T. and Marcarelli, A. M.: Cyanobacteria in Freshwater Benthic Environments, in: Ecology of Cyanobacteria II: Their Diversity in Space and Time, edited by: Whitton, B. A., Springer Netherlands, Dordrecht, 271–289, https://doi.org/10.1007/978-94-007-3855-3_9, 2012.

Singer, G. A., Fasching, C., Wilhelm, L., Niggemann, J., Steier, P., Dittmar, T., and Battin, T. J.: Biogeochemically diverse organic matter in Alpine glaciers and its downstream fate, Nature Geosci, 5, 710–714, https://doi.org/http://www.nature.com/ngeo/journal/v5/n10/abs/ngeo1581.html#supplementary-information, 2012.

Stedmon, C. A., Amon, R. M. W., Rinehart, A. J., and Walker, S. A.: The supply and characteristics of colored dissolved organic matter (CDOM) in the Arctic Ocean: Pan Arctic trends and differences, Marine Chemistry, 124, 108–118, https://doi.org/10.1016/J.MARCHEM.2010.12.007, 2011.

Tan, Q., Wang, X., Zheng, L., Wu, H., Xing, Y., Tian, Q., and Zhang, Y.: Anthropogenic pressure induced discontinuities of microbial communities along the river, Journal of Environmental Management, 373, 123764, https://doi.org/10.1016/j.jenvman.2024.123764, 2025.

Tanguang, G., Shichang, K., Cuo, L., Tingjun, Z., Guoshuai, Z., Yulan, Z., and Sillanpää, M.: Simulation and analysis of glacier runoff and mass balance in the Nam Co basin, southern Tibetan Plateau, Journal of Glaciology, 61, 447–460, https://doi.org/10.3189/2015JoG14J170, 2015.

Tedetti, M., Guigue, C., Mahieu, L., Martinot, P. L., Benavides, M., Dupouy, C., Nunige, S., Pulido-Villena, E., Dimier, C., Tilliette, C., Bonnet, S., Guieu, C., and Lefèvre, D.: Dissolved organic matter (DOC, CDOM, FDOM) in the western Tropical South Pacific: Depth- and subregion-resolved variability, and hydrothermal influence, Progress in Oceanography, 242, 103664, https://doi.org/10.1016/j.pocean.2025.103664, 2026.

Vannote, R. L., Minshall, G. W., Cummins, K. W., Sedell, J. R., and Cushing, C. E.: The river continuum concept, Canadian journal of fisheries and aquatic sciences, 37, 130–137, 1980.

Wang, B., Hu, K., Li, C., Zhang, Y., Hu, C., Liu, Z., Ding, J., Chen, L., Zhang, W., Fang, J., and Zhang, H.: Geographic distribution of bacterial communities of inland waters in China, Environmental Research, 249, 118337, https://doi.org/10.1016/j.envres.2024.118337, 2024.

Ward, N. D., Bianchi, T. S., Medeiros, P. M., Seidel, M., Richey, J. E., Keil, R. G., and Sawakuchi, H. O.: Where Carbon Goes When Water Flows: Carbon Cycling across the Aquatic Continuum, Frontiers in Marine Science, 4, https://doi.org/10.3389/fmars.2017.00007, 2017.

Wollheim, W. M., Harms, T. K., Robison, A. L., Koenig, L. E., Helton, A. M., Song, C., Bowden, W. B., and Finlay, J. C.: Superlinear scaling of riverine biogeochemical function with watershed size, Nat Commun, 13, 1230, https://doi.org/10.1038/s41467-022-28630-z, 2022.

Yin, H., Bao, Y., Huang, T., Zhang, Y., Sun, T., Tao, P., Sun, Q., and Chen, K.: Effects of cyanobacterial growth and decline on dissolved organic matter and endogenous nutrients release at the sediment–water interface, Carbon Res., 4, 40, https://doi.org/10.1007/s44246-025-00203-x, 2025.